ADVANCES IN ATMOSPHERIC SCIENCES, VOL. 25, NO. 4, 2008, 610–618

Improving the Vegetation Dynamic Simulation in a Land Surface Model by Using a Statistical-dynamic Canopy Interception Scheme

LIANG Miaoling[1,2] (梁妙玲) and XIE Zhenghui*[1] (谢正辉)

[1] *Institute of Atmospheric Physics, Chinese Academy of Sciences, Beijing* 100029

[2] *Graduate University of Chinese Academy of Sciences, Beijing* 100049

(Received 30 April 2007; revised 29 March 2008)

ABSTRACT

Canopy interception of incident precipitation, as a critical component of a forest's water budget, can affect the amount of water available to the soil, and ultimately vegetation distribution and function. In this paper, a statistical-dynamic approach based on leaf area index and statistical canopy interception is used to parameterize the canopy interception process. The statistical-dynamic canopy interception scheme is implemented into the Community Land Model with dynamic global vegetation model (CLM-DGVM) to improve its dynamic vegetation simulation. The simulation for continental China by the land surface model with the new canopy interception scheme shows that the new one reasonably represents the precipitation intercepted by the canopy. Moreover, the new scheme enhances the water availability in the root zone for vegetation growth, especially in the densely vegetated and semi-arid areas, and improves the model's performance of potential vegetation simulation.

Key words: canopy interception, vegetation dynamics, soil water, land surface model

DOI: 10.1007/s00376-008-0610-7

1. Introduction

The distribution and productivity of terrestrial vegetation are largely determined by soil moisture (Holdridge, 1974; Stephenson, 1990; Churkina et al., 1999; Ma and Osamu, 2002; Liu et al., 2005), which supplies water for vegetation transpiration and growth (Price and Carlyle-Moses, 2003; Cui et al., 2005). Canopy interception of incident precipitation, as a critical component of a forest's water budget, can affect the amount of water available to the understory and soil, and vegetation growth. It accounts for about 10%–30% of the annual precipitation on land, and varies greatly among different forest species, forest density, canopy structure, vegetation physiology, and climatic conditions (Wright et al., 1990; Whitehead and Kelliher, 1991; Thimonier, 1998; Kergoat, 1998; Zeng et al., 2005). Reasonable representation of canopy interception in a land surface model with a dynamic vegetation model is very important to improve its performance on vegetation simulation. The canopy interception scheme used in the Community Land Model with dynamic global vegetation model (CLM-DGVM) (Levis et al., 2004) overestimates the canopy interception, underestimates soil moisture for its excess canopy interception loss (Bonan et al., 2002; Bonan and Levis, 2006; Niu and Yang, 2005; Wang et al., 2005), and produces poor vegetation simulations (Levis et al., 2004; Bonan and Levis, 2006).

To improve the canopy interception representation of the model CLM-DGVM and its performance on vegetation simulation, we developed a statistical-dynamic approach which considers the interception amount dependent on vegetation species based on the statistics of observed canopy interception amount (Kergoat, 1998), the leaf area index (LAI) and stem area index (SAI) dynamic via the vegetation phenology to parameterize the canopy interception process, and implemented it into CLM-DGVM. Comparisons of simulations for vegetation biogeography, interception loss and soil moisture from CLM-DGVM with the new canopy interception scheme and the original one are presented to

*Corresponding author: XIE Zhenghui, zxie@lasg.iap.ac.cn

validate the model's performance in this paper.

2. Model development

The land surface model CLM-DGVM was developed by coupling the Community Land Model version 3 (CLM3) (Oleson et al., 2004) and the Lund-Potsdam-Jena Dynamic Global Vegetation Model (LPJ) (Sitch et al., 2003) to consider the two-way biogeophysical and biogeochemical feedbacks between vegetation and climate. Leaf area index is simulated by the model instead of being obtained from prescribed surface datasets and the vegetation distribution and coverage in CLM-DGVM are updated annually.

The original canopy interception scheme used in CLM-DGVM is described, and the statistical-dynamic interception scheme is developed in the section.

2.1 *The original canopy interception scheme in CLM-DGVM*

In the canopy interception scheme of original CLM-DGVM, the fraction of precipitation intercepted by vegetation $f_{\rm pi}$ is presented as a function of LAI and SAI as follows (Oleson et al., 2004):

$$f_{\rm pi} = 1 - \exp[-0.5({\rm LAI} + {\rm SAI})] \,, \tag{1}$$

where LAI is leaf area index and SAI is stem area index. And the precipitation intercepted by canopy $P_{\rm i}$ is given by

$$P_{\rm i} = f_{\rm pi} \cdot P \,, \tag{2}$$

where P is the incoming precipitation.

It follows from Eq. (1) and Fig. 1 that the scheme allows more than 30% of precipitation to be intercepted by the canopy when the LAI plus SAI is 0.72 $\rm m^2\ m^{-2}$ if the water storage in the canopy is less than its maximum storage capacity expressed as 0.1×(LAI+SAI) (mm) in the original CLM-DGVM (see Oleson et al., 2004). This is the case in growing seasons except in extremely arid regions of the world. If the water storage in the canopy does not exceed the maximum canopy storage capacity, which means all the intercepted water will subsequently evaporate, the canopy interception loss can be up to 90% or more when LAI plus SAI is greater than 4.6 $\rm m^2\ m^{-2}$. However, some studies showed that interception losses reach an average of 10%–35% of the annual precipitation in the world (Shuttleworth, 1989; Kelliher et al., 1993; Jarvish, 1993). Therefore, CLM-DGVM with the original canopy interception scheme overestimates canopy interception for most regions.

Table 1. Parameter in the statistical-dynamic canopy interception scheme.

Plant functional types	a
Temperate needle-leaved evergreen tree	0.06
Boreal needle-leaved evergreen tree	0.06
Boreal needle-leaved deciduous tree	0.06
Tropical broad-leaved evergreen tree	0.02
Temperate broad-leaved evergreen tree	0.02
Tropical broad-leaved deciduous tree	0.02
Temperate broad-leaved deciduous tree	0.02
Boreal broad-leaved deciduous tree	0.06
Temperate grass	0.01
Tropical grass	0.01

2.2 *The statistical-dynamic canopy interception scheme*

The canopy interception fraction of incident precipitation is expressed as a statistical proportion to LAI plus SAI following the approach of Kergoat (1998) which considers the interception to be proportional to LAI:

$$f_{\rm pi} = a \cdot ({\rm LAI} + {\rm SAI}) \,, \tag{3}$$

where the coefficient denotes a proxy for the precipitation regime effect dependent of Plant Function Type (PFT), which is given based on the observed interception amount according to Gerten et al. (2004) and shown in Table 1. The canopy interception fraction of incident precipitation for the scheme with three values of a is shown in Fig. 1. The maximum canopy storage capacity is taken as 0.1×(LAI+SAI) (mm) as described in Oleson et al. (2004).

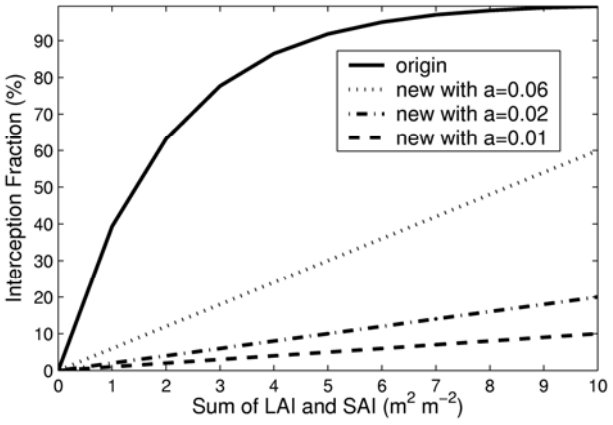

Fig. 1. Relations between the interception fraction and the sum of LAI and SAI in different canopy schemes. "origin" in legend stands for the origin scheme, and the other three legends stand for the new scheme with the parameter a as 0.06, 0.02 and 0.01, respectively.

For the sum of LAI and SAI 5 m^2 m^{-2}, the interception fraction of incident precipitation for the boreal needle-leaved evergreen forest from the new scheme is 30%, while that from the original scheme is 91.8%. The statistical-dynamic scheme developed above decreases the interception fraction, which is more reasonable according to the observations.

3. Data and experimental design

3.1 *Data*

A multiyear 3-hour atmospheric forcing dataset as CLM-DGVM required at a resolution of $0.5^\circ \times 0.5^\circ$ was created for the period 1961–2000 over continental China. The temperature, surface pressure, solar radiation, humidity and wind fields were derived from the 6-hour resolution NCEP (National Centers for Environmental Prediction) reanalysis data, which were provided by the Earth System Research Laboratory Physical Sciences Division in National Oceanic and Atmospheric Research from their web site at http://www.cdc.noaa.gov/. These NCEP data were regridded from their original $2.5^\circ \times 2.5^\circ$ grids to the $0.5^\circ \times 0.5^\circ$ grids using the bilinear interpolation method and then linearly interpolated to 3-hour resolution. The precipitation rates were derived from the observed daily precipitation data collected from 676 surface meteorology observation stations as follows: The station data were interpolated to $0.5^\circ \times 0.5^\circ$ grids using the inverse distance weighted interpolation method. To account for the effect of precipitation frequency, the 6-hour precipitation data were obtained by scaling to the total observed daily precipitation based on the diurnal variations of the 6-hour precipitation rate of NCEP reanalysis data, and then this 6-hour precipitation were averaged over the 6-hour interval and was applied uniformly to the two corresponding 3-hour intervals. We should mention that the coarse frequency of precipitation might have an impact on the canopy interception.

The land cover data over China with 1-km spatial resolution generated from the Moderate Resolution Image Spectroradiometer (MODIS) data (Li, 2004) was aggregated to $0.5^\circ \times 0.5^\circ$ resolution for comparison with the equilibrium potential vegetation in this paper. Because the crops and shrubs are not included in the model vegetation categories, we eliminated these two plants in the data. Observation data of soil moisture were obtained from Global Soil Moisture Data Bank (Robock et al., 2000; Li et al., 2005) (http://climate.envsci.rutgers.edu/soil_moisture/).

3.2 *Experimental design*

Two sets of model simulations during 1981 to 2000 were carried out to identify how the statistical-dynamic canopy interception scheme affects the vegetation biogeography simulated by CLM-DGVM with the new canopy interception scheme and the original one respectively. One is the simulation CTL by the original CLM-DGVM and the other one is the simulation EXP by the CLM-DGVM with the statistical-dynamic interception scheme. Initial conditions for each model mentioned were obtained from a 200-year spin-up simulation conducted from an initial condition of bare ground to reach an approximate equilibrium of vegetation cover, repeatedly driven with atmospheric data for the period from 1961 to 1990.

4. Results and discussion

The simulated vegetation biogeography, interception loss and soil water from the simulation EXP are compared with those from simulation CTL in this section.

4.1 *Vegetation biogeography*

Figure 2 compares the equilibrium vegetation distributions from the two simulations and the observed vegetation biogeography derived from 1-km MODIS land cover data (Li, 2004). Both simulations capture the broad patterns of vegetation distribution across continental China including the southern temperate broad-leaved evergreen forest, the northern broad-leaved deciduous forest, and the desert and grasses in northwestern China. Specifically, CLM-DGVM, with the new canopy interception scheme, successfully simulates the tropical broad-leaved evergreen forest in the Hainan Province and Taiwan Province, while the original CLM-DGVM does not. However, both models fail to capture the temperate needle-leaved evergreen forest in the southeastern coastland and the vast deserts of the Inner Mongolia Plateau. Discrepancies between the two simulations are also presented at the boundaries between the temperate broad-leaved evergreen forest and the temperate broad-leaved deciduous forest, and at the transition zone that lies between the temperate deciduous forest and the herbaceous steppe. As far as a visual comparison of the land cover over these areas, the simulation EXP is more consistent to the MODIS output than the simulation CTL.

The equilibrium vegetation geographic distribution patterns from the two simulations are quite similar (as Fig. 2 shows); however, comparison of the simulated vegetation coverage shows quite a difference in abundance (Fig. 3). In both simulations, grasses initially dominate and decline as trees grow, and vegetation distribution attains equilibrium in about 150 years. Forest coverage over continental China in the simulation EXP is higher than that in CTL. Figure 4 shows the

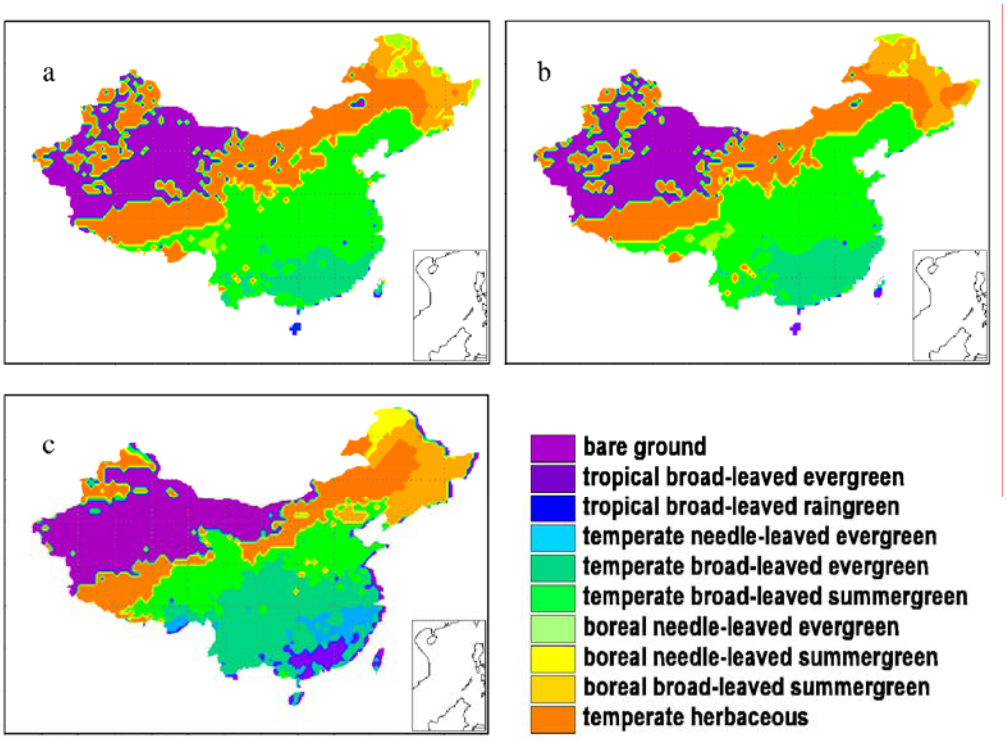

Fig. 2. Comparisons of simulated distributions of potential vegetation with that derived from MODIS data: (a) is the result from the simulation CTL with standard CLM-DGVM, (b) is that from the simulation EXP with modified canopy interception scheme, and (c) is that derived from the MODIS products offered by Li (2004) with crops and shrubs excluded.

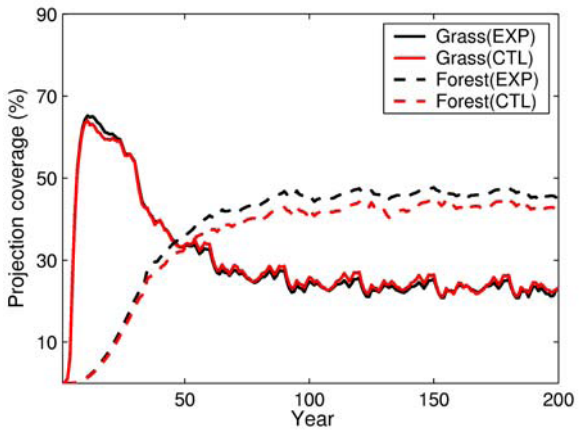

Fig. 3. Coverage of grassland and forest from the simulation CTL and EXP over 200 years from unvegetated land. ["Forest (CTL)", "Forest (EXP)", "Grass (CTL)" and "Grass (EXP)" in legend stand for forest coverage in simulation CTL and EXP, and grass coverage in simulation CTL and EXP, respectively.]

differences between the two simulations of vegetation coverage. In most regions of continental China, the simulation CTL estimates less forest coverage in favor of grasses, especially in the semi-arid areas which contain a transition zone from forest to steppe. In this transition zone, the dominant PFT is grass in simulation CTL, while it is temperate deciduous forest in EXP.

With respect to the coverage of potential vegetation, Houghton and Heckler (2003) estimated the coverage of natural forest over continental China as 45% from a map of natural ecosystem constructed from the predisturbance maps (Leemans, 1990; Matthews, 1983) and the natural regions described in Hou (1983). The forest coverage over continental China estimated from simulation EXP has a mean value of 44.7% during 1981 to 2000, which is much closer to Houghton's result mentioned above. In contrast, the value from simulation CTL is 40.9%.

To further quantify the effects of the modified scheme on vegetation simulation, we separate the study domain into 3 regions with different arid indices as shown in Fig. 5, which is derived from the annual precipitation and potential evapotranspiration (Ci, 1994). The mean coverage of forest and grass in different regions from CTL and EXP simulations are listed in Table 2. It shows that the significant difference occurs in the semiarid region, i.e. the mean forest coverage increases 9.6%, and grass coverage decreases 3%. In the wet region, coverage change is similar but much less than that in the semiarid region. This is

Table 2. NPP and vegetation coverage averaged in the 20 years from CTL and EXP simulations

Region	Grass coverage (%)		Forest coverage (%)		NPP (Pg C yr^{-1})	
Simulation	EXP	CTL	EXP	CTL	EXP	CTL
Arid region	19.87	16.7	0.01	0.0	0.118	0.074
Semi-arid region	54	57	25.0	15.4	0.73	0.58
Wet region	16.23	17.82	79.4	78.6	3.04	3.02

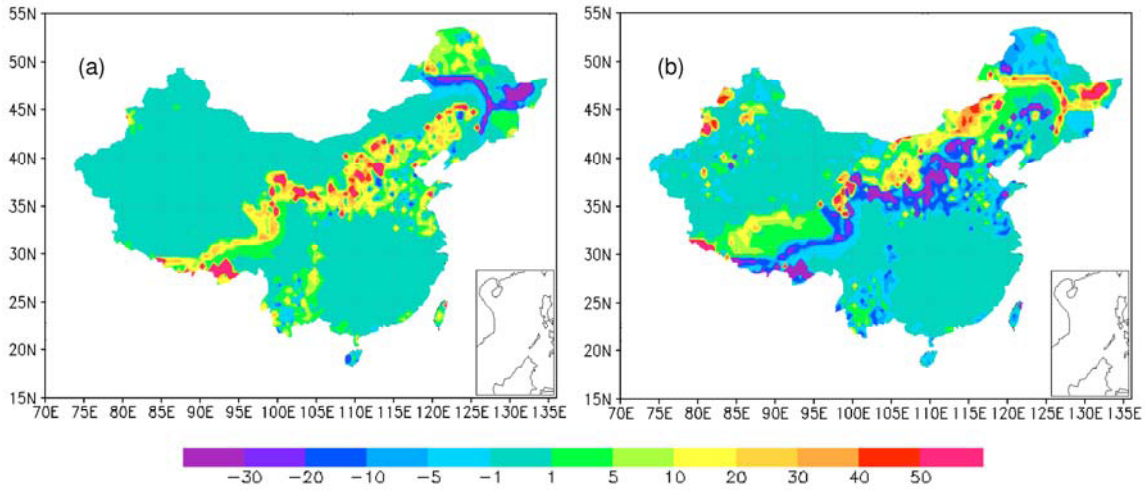

Fig. 4. Differences of vegetation cover as a percentage of the soil-covered portion of the grid cell from the simulation CTL and (EXP−CTL). (a) is for forest and (b) is for grass.

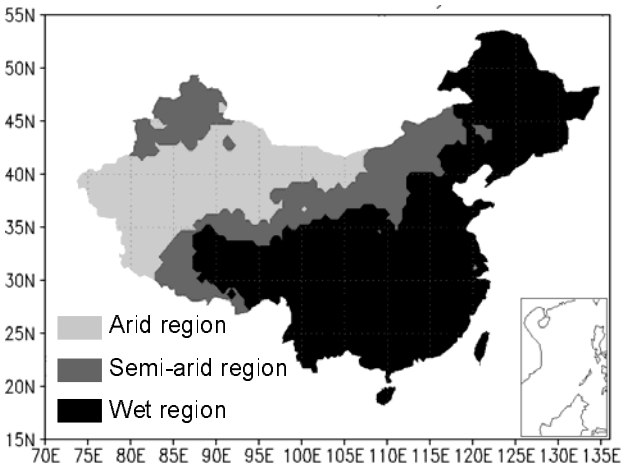

Fig. 5. Different regions over China based on the arid index.

reasonable because soil water in the wet region is sufficient for plant growth, which is not a limiting factor. In the arid region, grass coverage increases 3.17%, while the forest coverage changes little due to the extreme lack of precipitation.

4.2 *Canopy interception loss*

Independent observations of the interception loss from the broad-leaved evergreen forest of South China are used to provide insights as to which experiment (CTL vs EXP) is closer to reality (Fig. 6). Specifically, from a four-year measurement database at Dagangshan Mountain in Jiangxi Province (27.58°N, 14.67°E), the annual interception loss ratio in the area

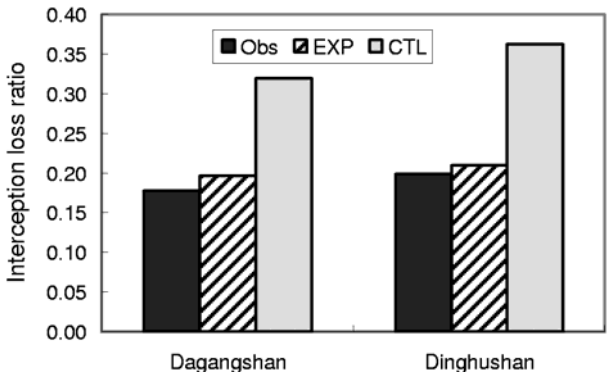

Fig. 6. Comparisons of simulated interception loss ratio with observation of two measurement sites. The legend "Obs" stands for observation.

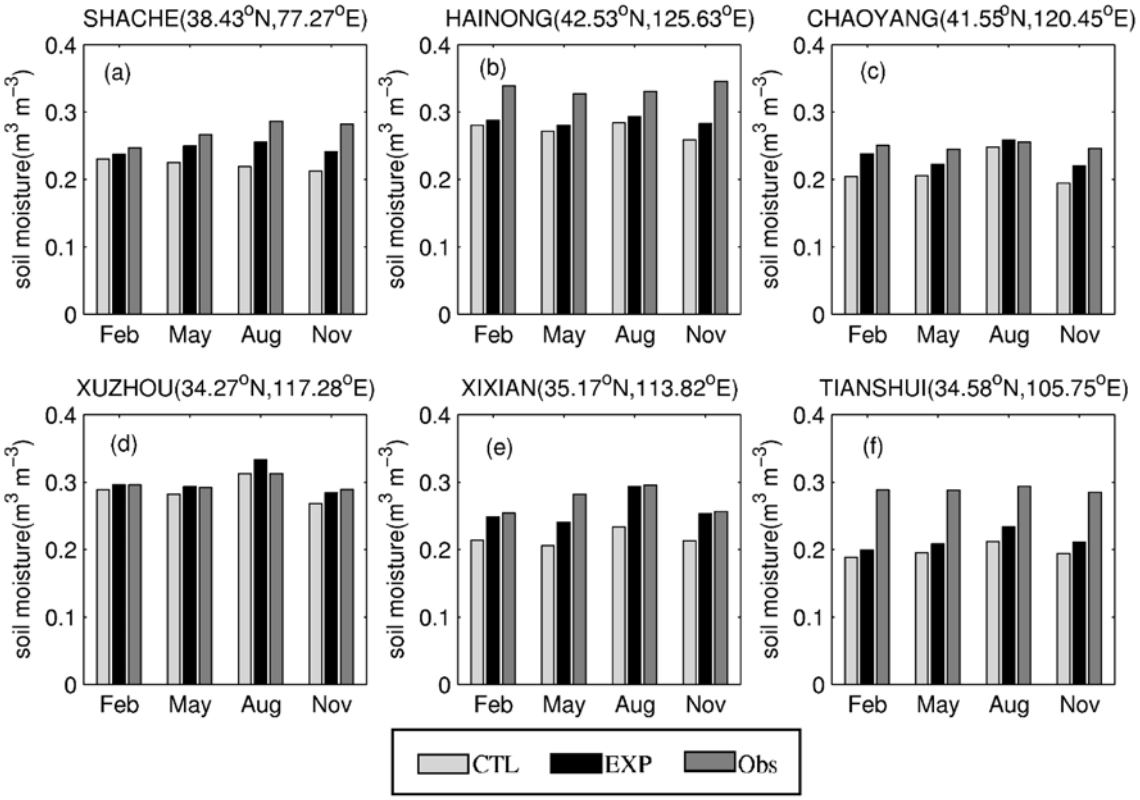

Fig. 7. Modeled mean monthly soil moisture in February, May, August and November for the top 50 cm layer in comparison with the observed data in (a) Northwest China, (b–c) North China and (d–f) Central China. Data are the average of the period from 1989 to 1999. ["Obs" in legend stands for observation data obtained from Global Soil Data Bank (Li et al., 2005)].

was found to be 0.178 (Cui et al., 2004). The simulated annual interception loss ratio at the closest model grid site (27.75°N, 114.75°E) are 0.320 and 0.197 for the simulation CTL and EXP, respectively. For another measurement site from Dinghushan Mountain of Guangdong Province (23.15°N, 112.5°E), the modeled annual interception loss ratio in the simulation EXP is 0.212 at the closest model grid (23.25°N, 112.25°E), which is close to the mean observed annual value (0.199) (Cui et al., 2004). In contrast, the corresponding value in the simulation CTL is 0.363, which diverges significantly from the observation. As noted by the above comparisons of interception loss, the simulation EXP is much closer to the observations than CTL, which indicates that the statistical-dynamic canopy interception scheme significantly improves the canopy interception amount in CLM-DGVM.

4.3 *Soil water*

Because the soil layer in the top 50 cm contains about 90% of the roots in the root zone in the model, we compare the soil moisture in the top 50 cm layer estimated in the simulations CTL and EXP with the observed soil moisture data of six measurement sites to validate the performance of the modified model regarding soil water (Fig. 7). Among the six sites, one is in northwestern China, two are located in northern China and the other three are in central China. The simulation EXP estimates wetter soil moisture and has less divergence from the observed than the CTL. The modified model significantly improves the magnitude of upper soil moisture over central China (Figs. 7d–f) and northwestern China (Fig. 7a). However, the magnitude of the improvement in northern China (Figs. 7b–c) is not as great as in central China and northwestern China.

Figure 8 shows the interannual variability of the simulated vegetation dynamic, vegetation evaporation (i.e., interception loss), transpiration and soil evaporation related to climatic variations in the semi-arid region from the simulation CTL and simulation EXP. The estimated net primary production is relative to precipitation in the environmental conditions and the correlation coefficients between them are 0.73 and 0.76 in CTL and EXP simulation, respectively. Both simulations indicate the same interannual patterns in

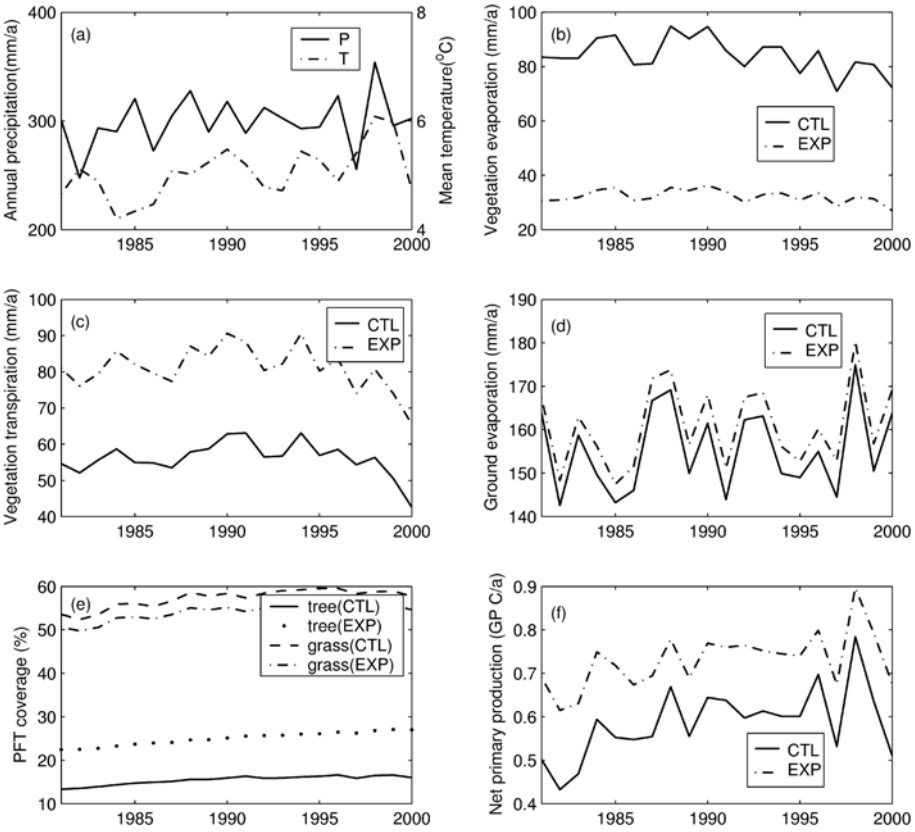

Fig. 8. (a) Interannual variability of climate including mean annual precipitation (mm a^{-1}) and temperature (°C), and (b) simulated annual vegetation evaporation, (c) transpiration and (d) soil evaporation and (e) vegetation coverage as well as (f) net primary production (f) from the simulation CTL simulation and EXP during 1981 to 2000 in the semi-arid region. ("T" in legend stands for mean temperature and "P" stands for precipitation, "CTL" and "EXP" stand for simulation CTL and simulation EXP respectively, and "tree(CTL)", "tree(EXP)", "grass(CTL)" and "grass(EXP)" stand for tree coverage in simulation CTL and EXP, grass coverage in simulation CTL and EXP respectively.)

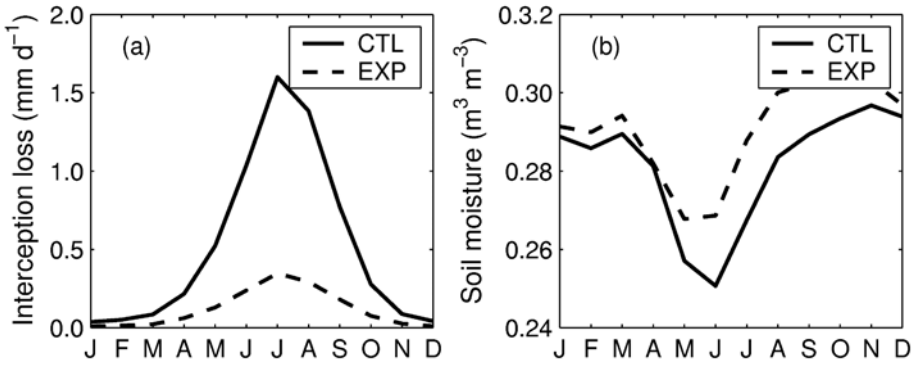

Fig. 9. Model estimated mean monthly (a) interception loss and (b) soil moisture of the top 50 cm from the simulation CTL and EXP over the transition zone (including model grids where the simulation bias in forest coverage is larger than 20% between the two simulations). Data are from the average of 20-year simulation ("CTL" and "EXP" in legend stand for simulation CTL and simulation EXP respectively).

water balance and vegetation variations. Since the statistical-dynamic canopy interception scheme decreases the interception amount and the vegetation evaporation largely relies on available water in the vegetation canopy, the modified model reduces the mean annual interception loss by 61.6% relative to that in CTL simulation (Fig. 8b), and thus increases the mean annual vegetation transpiration and ground evaporation by 44.5%, and 3.5% (Figs. 8c–d), respectively. The estimated mean evapotranspiration in simulation EXP is 7.2% less than that in CTL. Consequently, the simulation EXP estimates more vegetation coverage and net primary production because more water is available in the soil.

To emphasize the effect of the canopy interception scheme on soil water as well as on vegetation, we compare the simulated interception loss and soil moisture from both simulations over those regions where the difference of simulated forest coverage between the two simulations is larger than 20% (Fig. 9). The figure shows that the EXP simulation decreases the maximum interception loss in August from 1.65 mm d^{-1} to 0.5 mm d^{-1} (Fig. 9a). Correspondingly, the amount of precipitation reaching the ground increases and subsequently the soil moisture increases (Fig. 9b). The significant decrease of canopy interception loss and the increase of soil moisture during the growing season account for the increase of forest coverage.

5. Conclusions

A statistical-dynamic canopy interception scheme is developed and implemented into the land surface model CLM-DGVM to improve its vegetation simulation. The model with the statistical-dynamic canopy interception scheme is validated over continental China focusing on the vegetation biogeography, interception loss and soil water. The equilibrium potential vegetation from the simulation EXP with the new canopy interception scheme is more consistent to that derived from MODIS data than the CTL simulation with the original model. Moreover, the EXP simulation estimates 4% more forest coverage than CTL over continental China. Canopy interception loss and top 50 cm soil moisture from the simulation EXP are much closer to the *in-situ* observations than that from the simulation CTL. Comparisons of the two simulations for interception loss and soil moisture over the distinct bias region in the vegetation transition zone show that the new canopy interception scheme decreases interception loss significantly in rainy seasons and increases the soil water availability. It is concluded that the land surface model CLM-DGVM with the statistical-dynamic canopy scheme reasonably represents the precipitation intercepted by the canopy and the water availability in the root zone for vegetation transpiration, especially in the densely vegetated and semi-arid areas, and improves the model's performance the on potential vegetation simulation.

Acknowledgements. The authors would like to thank the Chinese Meteorology Administration (CMA) for providing observed precipitation and soil moisture data, and NCAR for offering the sources of CLM-DGVM as well as Dr. Li Guicai from CMA for providing the land cover data derived from the MODIS data. This work was supported by the CAS International Partnership Creative Group "The Climate System Model Development and Application Studies", the Knowledge Innovation Project of Chinese Academy of Sciences under Grant Nos. KZCX2-YW-217 and KZCX2-YW-126-2, and the National Basic Research Program under the Grant 2005CB321704. The authors thank the two anonymous reviewers for constructive comments and suggestions for this manuscript.

REFERENCES

Bonan, G. B., K.W. Oleson, M. Vertenstein, S. Levis, X. Zeng, Y. Dai, R. E. Dickinson, and Z. L. Yang, 2002: The land surface climatology of the Community Land Model coupled to the NCAR Community Climate Model. *J. Climate*, **15**, 3123–3149.

Bonan, G. B., and S. Levis, 2006: Evaluating aspects of the Community Land and Atmosphere Models (CLM3 and CAM3) using the CLM's dynamic global vegetation model. *J. Climate*, **19**, 2290–2301.

Churkina, G., S. W. Running, and A. L. Schloss, 1999: Comparing global models of terrestrial net primary productivity (NPP): The importance of water availability. *Global Change Biology*, **5**, 46–55.

Ci, L. J., 1994: Influence of global change on China's desertation. *Journal of Natural Resources*, **9**(4), 289–303. (in Chinese)

Cui, J. B., C. S. Li, and C. Trettin, 2005: Analyzing the ecosystem carbon and hydrologic characteristics of forested wetland using a biogeochemical process model. *Global Change Biology*, **11**, 278–289.

Cui, X. H., B. Wang, and Z. F. Deng, 2004: A study on eco-hydrological effect of evergreen broad-leaved forests in Dagangshan Mountain, Jiangxi Province. *Acta Agriculturae Universitatis Jiangxiensis*, **26**(5), 660–665. (in Chinese)

Gerten, D., S. Schaphoff, U. Haberlandt, W. Lucht, and S. Sitch, 2004: Terrestrial vegetation and water balance—hydrological evaluation of a dynamic global vegetation model. *J. Hydrol.*, **286**, 249–270.

Holdridge, L. R., 1974: Determination of world plant formations from simple climatic data. *Science*, **105**, 367–368.

Hou, X. Y., 1983: Vegetation of China with reference to its geographical distribution. *Annals of the Missouri*

Botanical Garden, **70**(3), 509–549.

Houghton, R. A., and J. L. Heckler, 2003: Sources and sinks of carbon from land-use change in China. *Global Biogeochemical Cycles*, **17**(2), 1034, doi:10.1029/2002GB 001970.

Jarvish, P. G., 1993: Water losses of crowns, canopies and communities, *Water Deficits-Plant Responses from Cell to Community*, Smith et al., Eds., Bios Scientific Publishers, Oxford, 285–315.

Kelliher, F. M., R. Leuning, and E. D. Schulze, 1993: Evaporation and canopy characteristics of coniferous forests and grasslands. *Oecologia*, **95**, 153–163.

Kergoat, L., 1998: A model for hydrological equilibrium of leaf area index on a global scale. *J. Hydrol.*, **212/213**, 268–286.

Leemans, R., 1990: Global data sets collected and compiled by the Biosphere Project, working paper. International Institute for Applied Systems Analyses. Laxenburg, Austria.

Levis, S., G. B. Bonan, M. Vertenstein, and K. W. Oleson, 2004: The community land model's dynamic global vegetation model (CLM-DGVM) technical description and user guide. NCAR Technical Note, May 2004, 50pp.

Li, G. C., 2004: Estimating the terrestrial net primary production in China based on the MODIS data and the efficiency of light energy utilization model. Ph. D. Dissertation, Institute of Remote Sensing Application, Chinese Academy of Sciences, 160pp. (in Chinese)

Li, H. B., A. Robock, S. X. Liu, X. G. Mo, and P. Viterbo, 2005: Evaluation of reanalysis soil moisture simulations using updated Chinese soil moisture observations. *Journal of Hydrometeorology*, **6**, 180–192.

Liu, S. K., S. D. Liu, Z. T. Fu, L. Sun, 2005: A nonlinear coupled soil-vegetation model. *Adv. Atmos. Sci.*, **22**(3), 337–342.

Ma, Y. M., and T. Osamu, 2002: *Combining Satellite Remote Sensing with Field Observations for Land Surface Heat Fluxes over Imhomogeneous Landscape.* China Meteorological Press, Beijing, 172pp. (in Chinese)

Matthews, E., 1983: Global vegetation and land use: New high resolution data bases for climate studies. *J. Climate Appl. Meteor.*, **22**, 474–487.

Niu, G. Y., and Z. L. Yang, 2005: A simple TOPMODEL-based runoff parameterization (SIMTOP) for use in global climate models. *J. Geophys. Res.*, **110** (D21106), doi:10.1029/2005JD006111.

Oleson, K. W., and Coauthors, 2004: Technical Description of the Community Land Model (CLM). NCAR Technical Note TN-461_STR, 174pp.

Price, A. G., and D. E. Carlyle-Moses, 2003: Measurement and modeling of growing season canopy water fluxes in a mature mixed deciduous forest stand, south Ontario, Canada. *Agricultural and Forest Meteorology*, **119**, 69–85.

Robock, A., Y. V. Konstantin, S. Govindarajalu, K. E. Jared, E. H. Steven, A. S. Nina, S. Liu, and A. Namkhai, 2000: The Global Soil Moisture Data Bank. *Bull. Amer. Meteor. Soc.*, **81**, 1281–1299.

Shuttleworth, W., 1989: Micrometeorology of temperate and tropical forest. *Philosophical Transactions of the Royal Society of London*, **B324**, 299–334.

Sitch, S., and Coauthors, 2003: Evaluation of ecosystem dynamics, plant geography and terrestrial carbon cycling in the LPJ dynamic global vegetation model. *Global Change Biology*, **9**, 61–185.

Stephenson, N. L., 1990: Climatic control of vegetation distribution: the role of the water balance. *The American Naturalist*, **135**, 649–670.

Thimonier, A., 1998: Measuring of atmospheric deposition under forest canopies: some recommendations for equipment and sampling design. *Environmental Monitoring and Assessment*, **52**, 353–387.

Wang, D. G., G. L. Wang, and E. A. Anagnostou, 2005: Use of satellite-based precipitation observation in improving the parameterization of canopy hydrological processes inland surface models. *Journal of Hydrometeorology*, **6**, 745–763.

Whitehead, D., and F. Kelliher, 1991: A canopy water balance model for a Pinus adiata stand before and after thinning. *Agricultural and Forest Meteorology*, **55**, 109–123.

Wright, R. F., B. J. Cosby, and M. B. Flaten, 1990: Evaluation of an acidification model with data from manipulated catchments in Norway. *Nature*, **343**, 53–55.

Zeng, G. M., G. Zhang, G. H. Huang, Y. M. Jiang, and H. L. Liu, 2005: Exchange of Ca^{2+}, Mg^{2+} and K^{+} and the uptake of H^{+}, NH^{+4} for the canopies in the subtropical forest influenced by the acid rain in Shaoshan forest located in central south China. *Plant Science*, **168**, 259–266.